Structural Chemistry (2021) 32:1279–1287
https://doi.org/10.1007/s11224-020-01698-3

ORIGINAL RESEARCH

Regioselective synthesis and DFT computational studies of novel β-hydroxy-1,4-disubstituted-1,2,3-triazole-based benzodiazepinediones using click cycloaddition reaction

Hossein Paghandeh[1] · Maryam Khalili Foumeshi[2] · Hamid Saeidian[1]

Received: 7 October 2020 / Accepted: 2 December 2020 / Published online: 7 January 2021

Abstract

Novel β-hydroxy-1,4-disubstituted-1,2,3-triazole-based benzodiazepinedione derivatives were synthesized by a regioselective cascade reaction and were fully characterized by HRMS, FT-IR, ^{1}H NMR, and ^{13}C NMR measurements. The cascade reaction consists of the azidation of epoxides and the Huisgen [3+2] dipolar cycloaddition of the resulted β-hydroxy azides with the *N*,*N*′-dipropargyl benzodiazepine to give the wished 1,2,3-triazole-based benzodiazepinedione derivatives. Good yields (60–85%), easily available and inexpensive starting materials, using water as a green solvent, and avoiding the handling of organic azides as they are generated in situ are the advantages of this method. Theoretical calculations were also conducted by the DFT method using the B3LYP functional and 6-31+G(d,p) basis set on structure to characterize structure **3a**. For structural and electronic characterization, ^{1}H and ^{13}C chemical shifts were calculated by the computational method and interpreted. The DFT calculated data were in line with the experimental data.

Keywords Benzodiazepine · Huisgen reaction · Azidation · DFT calculation · Electrophilicity index

Introduction

Diazepine nuclei are candidates for use in a wide range of drugs due to their anticoagulant, analgesic, sedative, and antifungal activities [1–5]. Most studies conducted on diazepines concern with the 1,5-benzodiazepine framework. Due to their wide range of biological properties, including their antioxidant, antiparasitic, anti-inflammatory, anti-Alzheimer's, and anti-anxiety activities, benzodiazepines have been of interest to chemists for the synthesis and conducting research on their analogues [6–9]. Clobazam, triclobazam, quetiapine, and olanzapine are used as benzodiazepine scaffold in the treatment of schizophrenia and mental disorders [10–12]. 1,5-Benzodiazepine scaffolds containing the triazole group have unique biological properties [13–17]. During the recent years, 1,2,3-triazoles have attracted much attention among the heterocyclic compounds due to their biological activities such as anti-HIV, antifungal, and anti-allergy activities as well as easy synthesis by the click method [18–20]. Anti-corrosion coatings, pigments, and ligand agents for measuring metals are some applications of the triazoles [21–24]. The thermal 1,3-dipolar cycloaddition reaction between alkynes and organic azides has been known for more than a century [25]. It has been shown that using the Cu(I) salts increases the cycloaddition reaction rate up to 10^{7} times and also leads to the formation of the regioselective 1,4-isomer as the dominant form [26]. Given that 1,2,3-triazoles have special pharmaceutical applications, the introduction of simple and effective methods for synthesizing the derivatives of these compounds can be very noteworthy. The organic azides are valuable intermediates in the organic synthesis [27]. Although nucleophilic substitution reaction of azide ion (N_3^-) with alkyl halides is introduced as one of the most efficient methods among the various ones of preparing azides, it has problems such as complexity and toxicity of the reactants, long times, difficult reaction conditions, and also low yields. Despite numerous reports released on the ring-opening reactions of the epoxides, to the best of the authors' knowledge, only a few studies deal with opening the epoxide rings using N_3^- [28]. Knowing the

✉ Hamid Saeidian
Saeidian1980@gmail.com

[1] Department of Science, Payame Noor University (PNU), P.O. Box 19395-4697, Tehran, Iran

[2] Faculty of Chemistry, Kharazmi University, P. O. Box 15719-14911, Tehran, Iran

history of the research group in the preparation of various triazole derivatives [29–36], a green, gentle, and effective method has been presented in this paper for the synthesis of β-hydroxy-1,4-disubstituted-1,2,3-triazole-based benzodiazepinediones in water (Scheme 1). In the present method, different types of epoxides were converted into β-hydroxyazides in a green, very practical, and simple method through reacting with sodium azide in water without increasing any catalyst or other additives with high efficiency and short time. After preparing the desired β-hydroxyazides, the final reaction step involves the synthesis of β-hydroxy-1,4-disubstituted-1,2,3-triazole-based benzodiazepinediones **3** via a cycloaddition of [4πs + 2πs] type in a copper(I)-catalyzed azide alkyne cycloaddition (CuAAC). In the final section of the study, density functional theory (DFT) calculations at the B3LYP/6-31+G(d,p) level have been undertaken on the characterized structure **3a** to obtain some of its physicochemical properties such as ^{1}H NMR and ^{13}C NMR data and electrophilicity index (Scheme 1).

Experimental and computational details

General information

All the chemicals required for the synthesis of β-hydroxy-1,4-disubstituted-1,2,3-triazole-based benzodiazepinediones **3** were supplied from Sigma-Aldrich, Fluka, and Merck companies. The all synthesized products were confirmed by spectroscopic data (Experimental section and supplementary information). A Bruker (DRX-400 Avance) NMR was used to record the ^{1}H and ^{13}C NMR spectra in $CDCl_3$ or acetone-d_6 at room temperature. FT-IR spectra were taken by a Nicolet spectrometer (Magna 550) using KBr pellets. High-resolution MS spectra (HRMS) were recorded on an LTQ Orbitrap XL using electrospray ionization (ESI) on a Waters Micromass AutoSpec Ultima. The reactions are monitored by thin-layer chromatography (TLC).

Computational details

The geometry of the considered structure **3a** is optimized at the DFT/B3LYP level with the 6-31+G(d,p) basis set using the Gaussian 09 software [37]. The structure was visualized in the GaussView 5.0 program. After geometry optimization and frequency calculation, zero-point energy (ZPE) and thermal correction are obtained at 298 K. NMR data calculations were performed using the gauge-independent atomic orbital (GIAO) method [38]. Relative chemical shifts were calculated by using the corresponding tetramethylsilane (TMS) shielding calculated at the same level of theory as the reference.

General synthesis procedure for β-hydroxy-1,4-disubstituted-1,2,3-triazole-based benzodiazepinediones 3

A total of 2.4 mmol sodium azide (0.117 g) was added to a stirred solution of 2.2 mmol of epoxide **1** in water (5 mL), and the resulting mixture was stirred at room temperature for 16 h. Dipropargyl benzodiazepine **2** (1 mmol, 0.225 g) and CuI

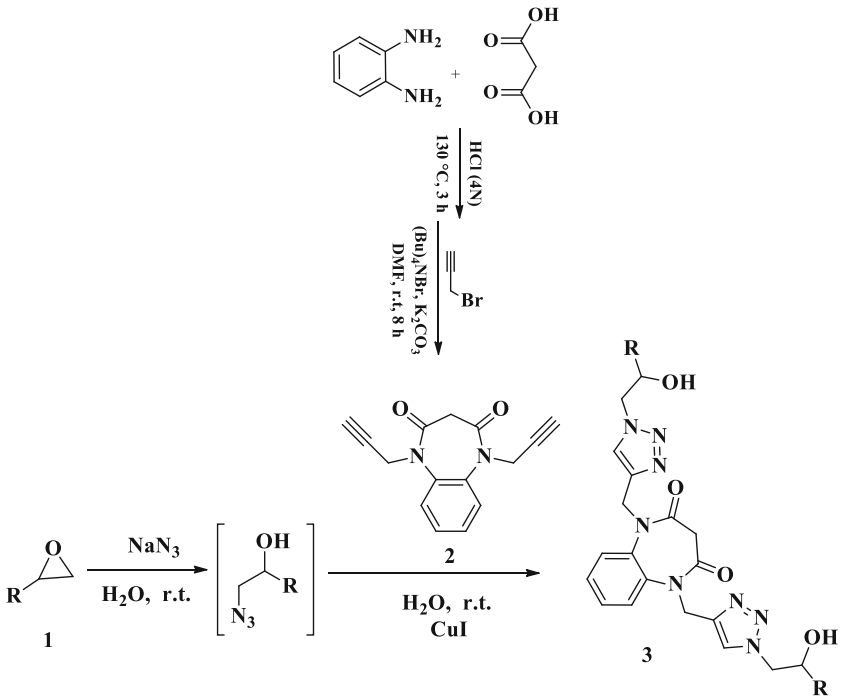

Scheme 1 General method for the efficient synthesis of β-hydroxy-1,4-disubstituted-1,2,3-triazole-based benzodiazepinediones **3**

(0.2 mmol, 0.038 g) were added to the reaction mixture, and the mixture was extracted at room temperature for 8 h. After the completion of the reaction (monitored by TLC), water (5 mL) was added to the reaction mixture and extracted with CH_2Cl_2 (3 × 5 mL) and then dried over Na_2SO_4. The crude was concentrated under vacuum and was purified by preparative TLC (eluent: ethyl acetate/methanol 2:1) to afford the desired products **3**.

Spectral data of the β-hydroxy-1,4-disubstituted-1,2,3-triazole-based benzodiazepinediones 3

3a: yellow solid; m.p.: 106–110 °C; FT-IR: 3675, 3612, 3412, 3157, 2952, 2936, 1690, 1667, 1599, 1551, 1501, 1459, 1432, 1368, 1081, 1051, 1034, 937, 412 cm^{-1}; ^1H NMR (400 MHz, acetone-d_6) δ: 7.91–7.72 (m, 4H), 7.31 (dd, J = 6.2, 3.5 Hz, 2H), 5.07–4.99 (m, 4H), 4.45–4.00 (m, 8H), 3.45 (dd, J = 12.2, 1.3 Hz, 1H), 3.16 (dd, J = 12.2, 1.1 Hz, 1H), 1.13 (dd, J = 9.3, 6.2 Hz, 6H); ^{13}C NMR (100 MHz, acetone-d_6) δ: 164.95, 143.18, 136.06, 126.55, 124.70, 123.80, 66.02, 56.77, 44.36, 43.35, 20.18; HRMS (ESI) exact mass calculated for $C_{21}H_{26}O_4N_8Na$: 477.19692, found: 477.19651. **3b**: white solid; m.p.: 140–143 °C; FT-IR: 464, 952, 1034, 1051, 1060, 1374, 1433, 1461, 1501, 1550, 1599, 1665, 1690, 2855, 2881, 2930, 2969, 3158, 3417, 3617 cm^{-1}; ^1H NMR (100 MHz, $CDCl_3$) δ: 7.72–7.61 (m, 3H), 7.45–7.20 (m, 3H), 5.29–4.82 (m, 4H), 4.46–4.33 (m, 2H), 4.25–4.08 (m, 2H), 4.05–3.86 (m, 3H), 3.33–3.21 (m, 2H), 1.54–1.37 (m, 4H), 1.03–0.82 (m, 7H); ^{13}C NMR (400 MHz, $CDCl_3$) δ: 165.34, 142.71, 135.48, 127.41, 125.49, 123.86, 71.57, 55.83, 43.99, 42.95, 27.52, 9.87; HRMS (ESI) exact mass calculated for $C_{23}H_{31}O_4N_8$: 483.24628, found: 483.24573. **3c**: yellow viscous liquid; FT-IR: 3616, 3402, 3157, 2959, 2934, 2874, 2863, 1689, 1666, 1599, 1550, 1501, 1460, 1433, 1380, 1660, 1502, 1036, 952, 24 cm^{-1}; ^1H NMR (400 MHz, $CDCl_3$) δ: 7.75–7.57 (m, 3H), 7.39–7.26 (m, 3H), 5.36–4.79 (m, 4H), 4.38 (dd, J = 16.5, 12.8 Hz, 2H), 4.23–3.94 (m, 4H), 3.29 (s, 2H), 1.54–1.20 (m, 14H), 0.89 (td, J = 7.1, 4.0 Hz, 6H); ^{13}C NMR (100 MHz, $CDCl_3$) δ: 165.42, 142.86, 135.52, 127.46, 125.73, 123.84, 69.96, 56.22, 44.22, 42.66, 34.23, 27.60, 22.56, 13.99; HRMS (ESI) exact mass calculated for $C_{27}H_{38}O_4N_8Na$: 561.29082, found: 561.29038. **3d**: yellow solid; m.p.: 155–160 °C; FT-IR: 478, 908, 1022, 1061, 1075, 1367, 1431, 1452, 1501, 1548, 1599, 1666, 1689, 2864, 2946, 3158, 3379, 3606 cm^{-1}; ^1H NMR (400 MHz, acetone-d_6) δ: 7.88–7.65 (m, 4H), 7.32 (d, J = 6.9 Hz, 2H), 5.13–4.95 (m, 4H), 4.31–4.16 (m, 3H), 3.91 (dt, J = 18.1, 10.2 Hz, 2H), 3.45 (d, J = 12.1 Hz, 1H), 3.16 (d, J = 12.1 Hz, 1H), 2.14–2.07 (m, 2H), 2.04–1.72 (m, 8H), 1.52–1.26 (m, 7H); ^{13}C NMR (100 MHz, acetone-d_6) δ: 164.85, 142.67, 136.20, 126.50, 123.85, 123.19, 72.09, 66.44, 44.35, 43.75, 34.79, 31.83, 24.70, 24.02; HRMS (ESI) exact mass calculated for $C_{27}H_{34}O_4N_8Na$: 557.25952, found: 557.25963. **3e**: yellow viscous liquid; ^1H NMR (400 MHz, $CDCl_3$) δ: 7.74–7.53 (m, 4H), 7.53–7.22 (m, 10H), 5.66–5.58 (m, 2H), 5.20–5.01 (m, 2H), 4.92–4.81 (m, 2H), 4.63–4.48 (m, 2H), 4.20–4.11 (m, 4H), 3.28 (s, 2H); ^{13}C NMR (100 MHz, $CDCl_3$) δ: 165.19, 142.79, 136.06,135.22, 129.08, 128.81, 127.19, 125.75, 125.17, 124.83, 67.29, 66.06, 64.61, 43.86; MS (ESI): 579 $[M + H]^+$; Anal. Calcd for $C_{25}H_{30}N_8O_2$: C, 63.35; H, 5.23; N, 19.37.O, 11.06, found: C, 63.43; H, 5.31; N, 19.43; O, 11.83. **3f**: yellow solid; m.p.: 127–133 °C; FT-IR: 3609, 3370, 3157, 2943, 2873, 1689, 1667, 1599, 1547, 1501, 1453, 1444, 1374, 1077, 1048, 998, 920, 461 cm^{-1}; ^1H NMR (400 MHz, $CDCl_3$) δ: 7.76–7.49 (m, 3H), 7.34–7.21 (m, 3H), 6.00–5.84 (m, 2H), 5.40–4.68 (m, 8H), 4.42–3.90 (m, 5H), 3.28 (dd, J = 5.3, 2.4 Hz, 2H), 2.75–2.62 (m, 2H), 2.32–1.60 (m, 13H); ^{13}C NMR (100 MHz, $CDCl_3$) δ: 165.25, 142.47, 140.37, 139.77, 135.50, 127.19, 123.92, 115.54, 72.40, 68.25, 66.72, 63.14, 44.40, 35.69, 28.41, 27.68; HRMS (ESI) exact mass calculated for $C_{31}H_{38}O_4N_8Na$: 609.29082, found: 609.29072. **3g**: white solid; m.p.: 132–135 °C; FT-IR: 3614, 3428, 3155, 2942, 2873, 1668, 1663, 1599, 1550, 1502, 1460, 1434, 1375, 1049, 1003, 917, 462 cm^{-1}; ^1H NMR (400 MHz, acetone-d_6) δ: 7.81 (dd, J = 6.2, 3.5 Hz, 2H), 7.72 (s, 2H), 7.31 (dd, J = 6.2, 3.5 Hz, 2H), 5.93–5.78 (m, 4H), 5.06 (s, 4H), 4.99 (dt, J = 5.9, 1.2 Hz, 4H), 4.07 (t, J = 4.1 Hz, 4H), 4.00 (q, J = 5.6 Hz, 2H), 3.46 (d, J = 12.1 Hz, 1H), 3.16 (d, J = 12.2 Hz, 1H); ^{13}C NMR (100 MHz, acetone-d_6) δ: 165.00, 143.65, 135.96, 135.68, 126.61, 123.82, 123.50, 123.14, 61.20, 51.17, 44.37, 43.50; HRMS (ESI) exact mass calculated for $C_{23}H_{25}O_4N_8$: 477.20042, found: 477.20037. **3h**: yellow solid; m.p.: 115–120 °C; FT-IR: 3617, 3391, 3157, 2944, 2851, 1689, 1665, 1599, 1550, 1501, 1459, 1433, 1370, 1060, 1051, 1021, 885, 462 cm^{-1}; ^1H NMR (400 MHz, $CDCl_3$) δ: 7.73–7.57 (m, 3H), 7.38–7.27 (m, 3H), 5.89–5.72 (m, 2H), 5.37–4.80 (m, 8H), 4.45–4.33 (m, 2H), 4.26–3.90 (m, 5H), 3.63 (dd, J = 52.2, 4.7 Hz, 1H), 3.30 (d, J = 1.7 Hz, 2H), 2.35–2.10 (m, 4H), 1.65–1.47 (m, 4H); ^{13}C NMR (100 MHz, $CDCl_3$) δ: 165.32, 142.68, 137.82, 135.52, 127.29, 125.22, 123.92, 115.41, 69.54, 56.17, 44.21, 42.58, 33.42, 29.67; HRMS (ESI) exact mass calculated for $C_{27}H_{34}O_4N_8Na$: 557.25952, found: 557.25908. **3i**: yellow viscous liquid; ^1H NMR (400 MHz, $CDCl_3$) δ: 7.62–7.59 (m, 3H), 7.28–7.18 (m, 3H), 4.98–4.90 (m, 2H), 4.47–4.14 (m, 6H), 3.96–3.23 (m, 12H), 1.52–1.39 (m, 4H), 1.34–1.21 (m, 6H), 0.88–0.82 (m, 8H); ^{13}C NMR (100 MHz, $CDCl_3$) δ: 165.16, 142.96, 139.13, 130.91, 127.17, 125.27, 71.77, 69.04, 58.09, 53.34, 44.44, 38.65, 31.57, 19.21, 19.18, 14.05; MS (ESI): 613 $[M + H]^+$. **3j**: yellow viscous liquid; ^1H NMR (400 MHz, $CDCl_3$) δ: 7.80–7.67 (m, 4H), 7.30–7.16 (m, 2H), 5.02–4.98 (m, 3H), 4.50–4.23 (m, 5H), 4.10–4.08 (m, 2H), 3.53–3.16 (m, 10H), 1.18–0.81 (m, 12H); ^{13}C NMR (100 MHz, $CDCl_3$) δ: 165.18, 142.97, 135.40, 127.18, 125.68, 123.82, 72.37, 69.28, 62.01, 53.22, 44.47, 44.09, 43.61, and 21.99; MS (ESI): 571 $[M + H]^+$. **3k**: colorless

viscous liquid; FT-IR: 3671, 3575, 3382, 3158, 2954, 2867, 1689, 1666, 1599, 1548, 1501, 1454, 1433, 1367, 1113, 1081, 1050, 952, 462 cm^{-1}; ^1H NMR (400 MHz, acetone-d_6) δ: 7.87–7.82 (m, 2H), 7.80–7.74 (m, 2H), 7.40–7.25 (m, 12H), 5.14–5.03 (m, 4H), 4.63–4.49 (m, 8H), 4.47–4.36 (m, 2H), 4.20 (*t*, *J* = 7.90 Hz, 2H), 3.53–3.41 (m, 5H), 3.18 (dd, *J* = 12.1, 1.0 Hz, 1H); ^{13}C NMR (100 MHz, acetone-d_6) δ: 166.02, 144.30, 139.69, 137.11, 129.33, 128.71, 128.53, 127.67, 126.01, 124.93, 74.01, 72.84, 70.12, 54.16, 45.44, 44.58; HRMS (ESI) exact mass calculated for $C_{35}H_{38}O_6N_8Na$: 689.28065, found: 689.28047. **3l**: orange viscous liquid; FT-IR: 3570, 3407, 3157, 2952, 2912, 2865, 1689, 1666, 1599, 1550, 1502, 1460, 1432, 1365, 1112, 1061, 1051, 880, 409 cm^{-1}; ^1H NMR (400 MHz, acetone-d_6) δ: 7.88–7.72 (m, 4H), 7.32 (dd, *J* = 6.1, 3.5, 2H), 5.91 (dd, *J* = 17.2, 10.6 Hz, 2H), 5.28 (dq, *J* = 17.3, 1.8 Hz, 2H), 5.17–5.04 (m, 6H), 4.61–4.44 (m, 4H), 4.44–4.31 (m, 2H), 4.15 (dd, *J* = 13.3, 7.7 Hz, 2H), 4.00 (dq, *J* = 5.5, 1.3 Hz, 4H), 3.50–3.31 (m, 5H), 3.17 (dt, *J* = 12.1, 1.2 Hz, 1H); ^{13}C NMR (100 MHz, acetone-d_6) δ: 164.91, 143.20, 136.04, 135.12, 126.57, 124.90, 123.82, 115.90, 71.82, 69.08, 53.05, 44.35, 43.49, 43.27; HRMS (ESI) exact mass calculated for $C_{27}H_{34}O_6N_8Na$: 589.24935, found: 589.24898.

Results and discussion

Synthesis of the β-hydroxy-1,4-disubstituted-1,2,3-triazole-based benzodiazepinediones 3

The starting material dipropargyl benzodiazepine **2** is readily prepared from the commercial available o-phenylenediamine in high yield (70–80%) and excellent purity in-house [32]. With the dipropargyl benzodiazepine **2** in hand, attention was focused on copper(I)-catalyzed azide alkyne cycloaddition (CuAAC) **2** to produce the β-hydroxy-1,4-disubstituted-1,2,3-triazole-based benzodiazepinediones **3**. We began our investigation with the reaction of 2-methyloxirane **1a** (2.2 mmol), sodium azide (2.4 mmol), and dipropargyl benzodiazepine **2** (1 mmol) as a model reaction. Screening of solvents indicated that water is the best choice, affording the desired product **3a** up to 50% yield (Table 1, entries 1–3). Undoubtedly, water is one of the greenest solvents in the organic synthesis due to its cheapness, availability, and safety in terms of the work and environment.

The model reaction was performed in the presence of Sharpless catalytic system in water (Table 1, entry 2). Using copper(II) acetate in the presence of sodium ascorbate for an in situ reduction, a good degree of conversion to the desired product **3a** was observed (80%). The yield was decreased to 51% when CuCl was used as the copper source (Table 1, entry 3). No better yields were obtained when organic solvents or the mixture system such as EtOH, DMSO, *t*-BuOH, and H_2O/t-BuOH (1:1) was used (Table 1, entries 4–8). Optimal reaction conditions were determined to be CuI (10 mol%) as the catalyst and water as the solvent at room temperature for 8 h (Table 1, entry 1). With the optimized reaction conditions in hand, we next explored the scope of the CuAAC reaction of dipropargyl benzodiazepine **2** with different types of epoxide derivatives **1a-l**, giving rise to the corresponding β-hydroxy-1,4-disubstituted-1,2,3-triazole-based benzodiazepinediones **3** in good to excellent yields (Fig. 1).

Table 1 Optimization conditions for the model reaction of dipropargyl benzodiazepine **2**, NaN_3, and 2-methyloxirane **1a**

Entry	Catalyst	Solvent	Yield (%)[a]
1	CuI	H_2O	82
2[b]	$Cu(OAc)_2$	H_2O	80
3	CuCl	H_2O	51
4	CuI	H_2O/EtOH (1:1)	42
5	CuI	t-BuOH	Trace
6	CuI	H_2O/t-BuOH (1:1)	18
7	CuI	PEG400	37
8	CuI	DMSO	Trace

[a] Reaction conditions: 2-methyloxirane **1a** (2.2 mmol), sodium azide (2.4 mmol), dipropargyl benzodiazepine **2** (1 mmol), catalyst (10 mol%), solvent (5 mL), r.t., 8 h

[b] The reaction was performed in the presence of sodium ascorbate (10 mol%)

It should be noted that the corresponding β-hydroxy-1,4-disubstituted-1,2,3-triazole-based benzodiazepinediones **3** were synthesized as a single regioisomer in excellent yields. As would be observed from Fig. 1, the product of the styrene oxide (**3e**) formed exclusively by the attack of the azide ion at benzylic carbon of styrene oxide, due to the stabilization of the partial positive charge by the phenyl ring (electronic interaction is dominated over steric hindrance). However, other epoxide derivatives, despite the presence of Cu(I) Lewis acid, gave single regioisomers with preferential attack at the less hindered terminal carbon atom, which was confirmed by the reported literature [31, 39]. The structure of all desired products **3a-3l** was confirmed by FT-IR, ^1H NMR, ^{13}C NMR, and HRMS (ESI) analysis (Experimental section and supplementary information). As a representative example, ^1H NMR and ^{13}C NMR spectra of **3a** are discussed in the following section (computation section) and compared with the DFT calculated data.

DFT studies on the structure of β-hydroxy-1,4-disubstituted-1,2,3-triazole-based benzodiazepinedione 3a

DFT is a quantum computational modeling technique utilized in chemical, physical, and material sciences to investigate the

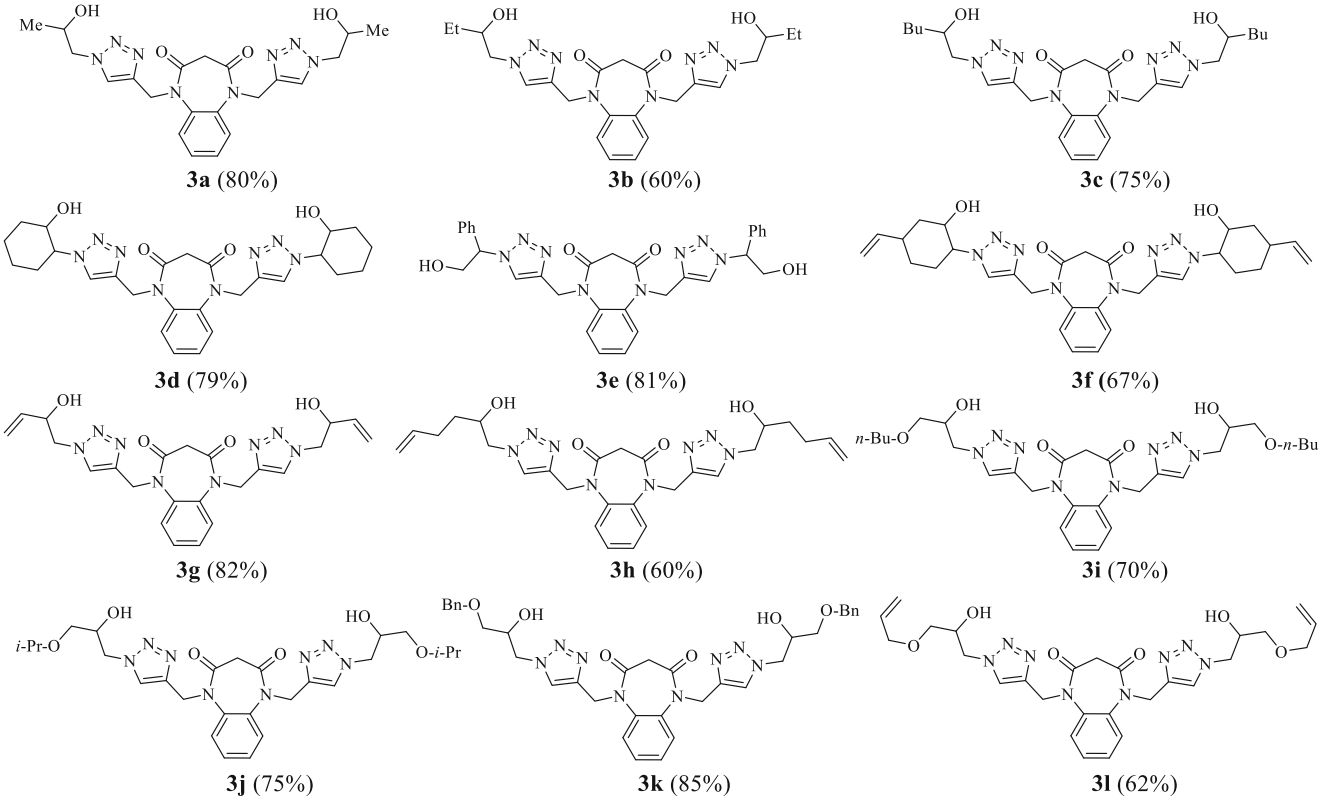

Fig. 1 Chemical structures of synthesized β-hydroxy-1,4-disubstituted-1,2,3-triazole-based benzodiazepinediones **3**

structural/electronic data of atoms, molecules, and condensed phases. Nowadays, it is widely accepted that DFT methods provide a valuable and in some cases the only alternative to obtain accurate physicochemical properties of organic molecules. On the other hand, it has been found that the hybrid functional B3LYP provides a good balance between placed and localized bond structures. It has emerged as a good compromise in computational cost and accuracy in results. Recently, the performance of DFT methods in the calculation of NMR properties has also been the subject of many theoretical studies. With the encouraging experimental data of the β-hydroxy-1,4-disubstituted-1,2,3-triazole-based benzodiazepinedione derivatives **3**, attention was focused on DFT calculations of the characterized product **3a** to obtain its physicochemical data such as structural and electronic data, HOMO-LUMO analysis, and spectral data calculations. Optimized geometry of **3a** by using the B3LYP/6-31+G(d,p) method is shown in Fig. 2.

The representative calculated bond lengths and bond angles of **3a** are listed in Table 2. All bond lengths and bond angles are in the normal range. The bond lengths C=O and C-O were found to be 1.228 and 1.424 Å, respectively. The bond length in triazole ring was calculated as 1.365 Å for single-bonded N^{49}=C^{52}atoms. The C^{1}-C^{2}-C^{3} and C^{55}-N^{27}-N^{50} angles in the phenyl and triazole ring are 119.7 and 110.4°, respectively. In the carbonyl group, N^{11}-C^{13}-O^{16} was calculated as 122.7°.

Structural analysis of compound **3a** revealed the presence of two noncovalent intramolecular H-bond interactions. Strong intramolecular hydrogen bonding was observed in **3a** [H^{59}…N^{50}, 2.022 Å] with the hydrogen atom (H^{59}) in the hydroxyl group as a donor and the nitrogen atom (N^{50}) in the triazole ring as an acceptor. On the other hand, a weak intermolecular C-H bonding (2.743 Å) was also observed with the hydrogen atom (H^{57}) in the triazole ring and the nitrogen atom (N^{51}) in other triazole ring (Fig. 2).

Calculated total energy, dipolar moment, and electronic data such as electrophilicity for **3a** in gas phase by using the B3LYP/6-31+G(d,p) method are collected in Table 3. The dipole moment (μ_D) is an important parameter of the electronic distribution in a molecule, which can be related to the interaction strength of molecules and metal. The dipole moment value of **3a** is 5.1 D.

The gap between the highest occupied molecular orbital (HOMO) and the lowest unoccupied molecular orbital (LUMO) energy levels (E_g) of an organic molecule was an important parameter that determined the reactivity of the molecule and stability index [40]. As E_g decreases, the reactivity of the molecule increases, leading to a decrease in the stability of the molecule [41]. E_g is the energy gap between HOMO and LUMO and is calculated as Eq. (1):

$$E_g = E_{HOMO} - E_{LUMO} \quad (1)$$

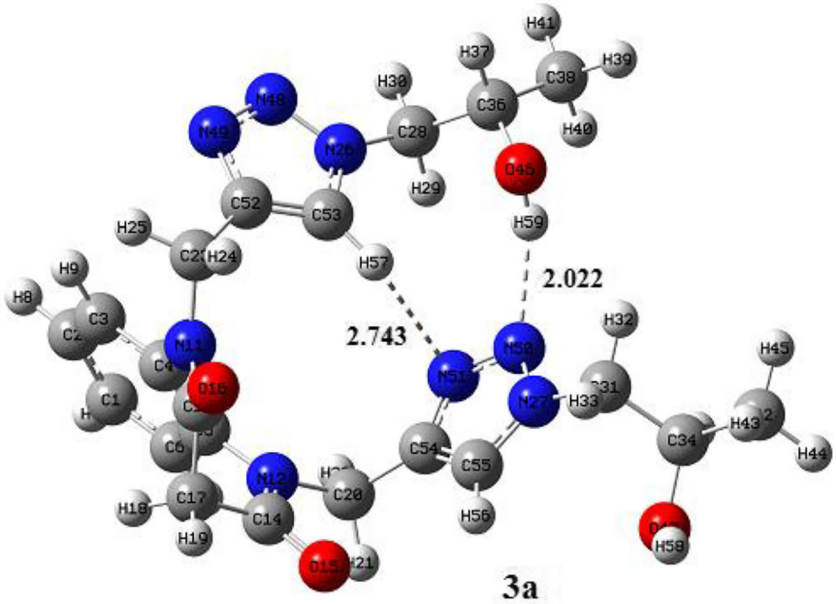

Fig. 2 The B3LYP/6-31+G(d,p) optimized geometry of **3a** (distance in Å)

where E_{LUMO} is the energy of LUMO and E_{HOMO} is the energy of HOMO. The energy gap of **3a** was found to be 0.137 eV. According to the molecular orbital theory, the HOMO and LUMO orbitals are the most important factors affecting the bioactivity of organic compounds. Topologies of HOMO and LUMO orbitals of **3a** are demonstrated in Fig. 3. As can be seen in Fig. 2, LUMO electron clouds were located mainly in the benzodiazepine ring and not in the triazole rings. The HOMO orbital having the energy levels of − 0.335 eV is localized on triazole rings and benzodiazepine ring.

The hardness and softness are commonly used as criteria of chemical reactivity and stability. The hardness (η) can be estimated from the calculated HOMO and LUMO energies. The smaller value of hardness implies higher reactivity. A molecule with a small HOMO-LUMO gap is more reactive. The hardness value of **3a** is 0.098 eV. Electrophilicity index (ω) as a fundamental object of organic compounds is calculated according to Eq. (2) [42]:

$$\omega = \mu^2/2\eta \quad (2)$$

$$\mu = (\mathrm{ELUMO} + \mathrm{EHOMO})/2 \text{ and} \quad (3)$$

$$\eta = (\mathrm{ELUMO–EHOMO})/2$$

where μ and η are the chemical potential and chemical hardness, respectively, given by Eq. (3). The electrophilicity index of **3a** equals to 0.520 eV.

The experimental ^{1}H NMR spectrum of **3a** consisted of a multiple signal at $\delta = 1.13$ ppm for methyl groups, an ABdd system ($J = 12.2$, 1.1 Hz) at $\delta = 3.16$–3.45 ppm for two methylene protons in benzodiazepine ring, some multiple signals (12 protons) at $\delta = 4.00$–5.07 ppm for methylene and methine groups, two signals for benzene protons at $\delta = 7.31$ and 7.72 ppm, and one characteristic triazole protons at $\delta =$ 7.91 ppm. The ^{1}H-decoupled ^{13}C NMR spectrum of **3a** showed 11 resonances, which is in agreement with the proposed structure, with the amide carbon appearing at $\delta =$

Table 2 The representative B3LYP/6-31+G(d,p) calculated bond lengths and bond angles of **3a**

Atom groups	Bond lengths (Å)	Atom groups	Bond angles (°)
O^{47}-C^{34}	1.428	C^{34}-O^{47}-H^{58}	109.2
N^{11}-C^{23}	1.483	C^{55}-N^{27}-N^{50}	110.4
N^{49}-C^{52}	1.365	O^{16}-C^{13}-N^{11}	122.7
C^{54}-C^{55}	1.384	N^{51}-C^{54}-C^{20}	121.5
C^{13}-C^{17}	1.526	H^{33}-C^{31}-H^{32}	108.2
C^{28}-C^{36}	1.538	C^{36}-O^{46}-H^{59}	110.3
C^{31}-H^{33}	1.095	N^{27}-N^{50}-N^{51}	107.7
C^{53}-H^{57}	1.075	H^{39}-C^{38}-H^{40}	108.4
C^{3}-C^{4}	1.405	C^{3}-C^{4}-C^{5}	118.8

Table 3 The calculated electronic data of **3a** by the B3LYP/6-31+G(d,p) computational method

Parameter	Value
Energy (Hartree)	1554.8
μ_D (Debye)	5.1
E_{HOMO} (eV)	− 0.335
E_{LUMO} (eV)	− 0.198
E_g (eV)	0.137
Chemical potential (μ) (eV)	− 0.266
Chemical hardness (η) (eV)	0.068
Electrophilicity (ω) (eV)	0.520

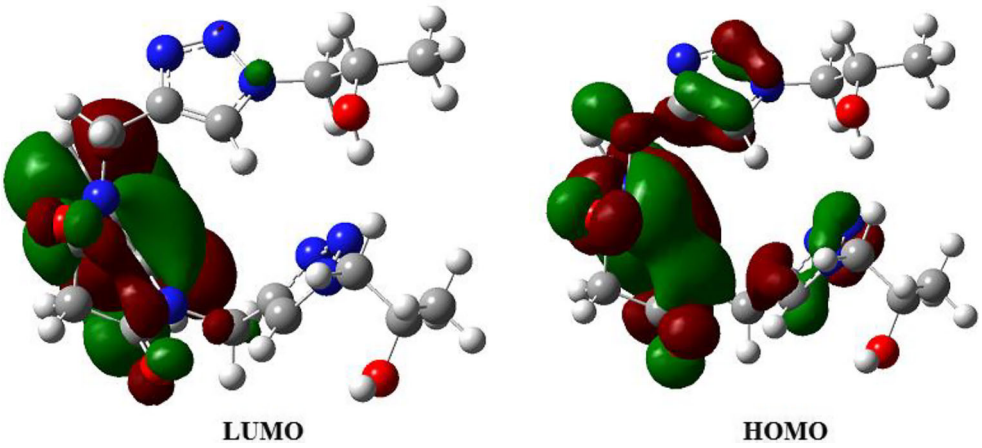

Fig. 3 Molecular orbitals of HOMO and LUMO for **3a**

164.95 ppm, 5 distinct resonances for the aromatic carbons of benzene and triazole groups between $\delta = 123.80$ and 143.18 ppm, and five resonances at $\delta = 20.18$–66.02 ppm for aliphatic carbons. Calculated GIAO ^{1}H and ^{13}C chemical shift values (regarding TMS) of **3a** by using the B3LYP/6-31+G(d,p) method and experimental results in acetone-d_6 as NMR solvent are tabulated in Table 4.

As mentioned, the experimental NMR spectra have been carried out in acetone-d_6 as solvent; therefore, the calculated NMR data for optimized geometry **3a** were also obtained by 6-31+G(d,p) basis set in acetone-d_6. We have employed solvent effects into account by using the conductor-like polarizable continuum model through the DFT calculations done at B3LYP/6-31+G(d,p) level of theory. The correlations of ^{1}H and ^{13}C NMR data in acetone for 6-31+G(d,p) basis set are shown in Fig. 3. The calculated ^{1}H and ^{13}C chemical shifts are in good agreement with the experimental data. Plots of experimental vs computed ^{1}H NMR chemical shifts and experimental vs computed ^{13}C NMR chemical shifts (Fig. 4) indicate linear relationships with $r^2 = 0.993$ and $r^2 = 0.998$, respectively.

In the ^{1}H NMR spectrum of **3a**, the chemical shift values of the methyl protons were observed to be 1.15 ppm, whereas this signal has been calculated as 1.84 ppm. The experimental chemical shifts of methylene protons in benzodiazepine ring were observed at $\delta = 3.85$ ppm, whereas the computed ^{1}H NMR chemical shifts of corresponding signals were found at $\delta =$ 3.47 ppm. ^{13}C NMR spectrum of **3a** shows a signal at 164.95 ppm, due to the carbon of the carbonyl group. This signal is calculated as 166.07 ppm for B3LYP levels. The most deviation is observed in the ^{13}C chemical shift of carbons 36 and 34 of **3a**, 66.02 ppm, whereas it was calculated as 75.65 ppm.

Table 4 ^{1}H and ^{13}C chemical shifts in acetone-d_6 for **3a**

Atom[a]	δ_{B3LYP} (ppm)	δ_{exp} (ppm)	δ_{exp}-δ_{B3LYP}
$H^{7, 8}$	8.17	7.76	0.41
$H^{43, 44, 45, 41, 40, 39}$	1.84	1.15	0.68
$H^{21, 22, 24, 25}$	5.91	5.07	0.84
$H^{18, 19}$	3.85	3.47	0.38
$H^{9, 10}$	8.30	7.86	0.44
$H^{35, 37}$	4.59	4.39	0.20
$H^{57, 56}$	8.20	7.82	0.62
$H^{33, 32, 30, 29}$	4.93	4.42	0.51
$C^{14, 13}$	166.07	164.95	1.12
$C^{20, 23}$	49.54	44.36	5.18
$C^{38, 42}$	25.94	20.18	5.76
$C^{54, 52}$	146.10	143.18	2.92
$C^{5, 4}$	138.46	136.06	2.40
$C^{55, 53}$	127.41	126.55	0.86
$C^{3, 6}$	124.70	123.80	0.90
$C^{1, 2}$	126.66	124.70	1.96
$C^{36, 34}$	75.65	66.02	9.63
$C^{28, 31}$	62.45	56.77	5.68
C^{17}	50.07	43.35	6.72

[a] For numbering of atoms, refer to Fig. 2

Conclusions

In this research, for the first time, a simple method has been introduced for the synthesis of the β-hydroxy-1,4-disubstituted-1,2,3-triazole-based benzodiazepinediones **3** as raw materials from dipropargyl benzodiazepine and through the azidation of epoxides and then the Cu(I)-catalyzed azide-alkyne cycloaddition reaction in mild and green conditions (room temperature and water as solvent) without any by-products. It can be claimed that the present method is an environmentally friendly approach and acceptable one in terms of observing the principles of the green chemistry and click synthesis. Then, the DFT calculations were performed on one of the derivatives prepared in order to obtain the physicochemical characteristics such as NMR data and HOMO-LUMO analysis. The structure of **3a** was fully optimized by using

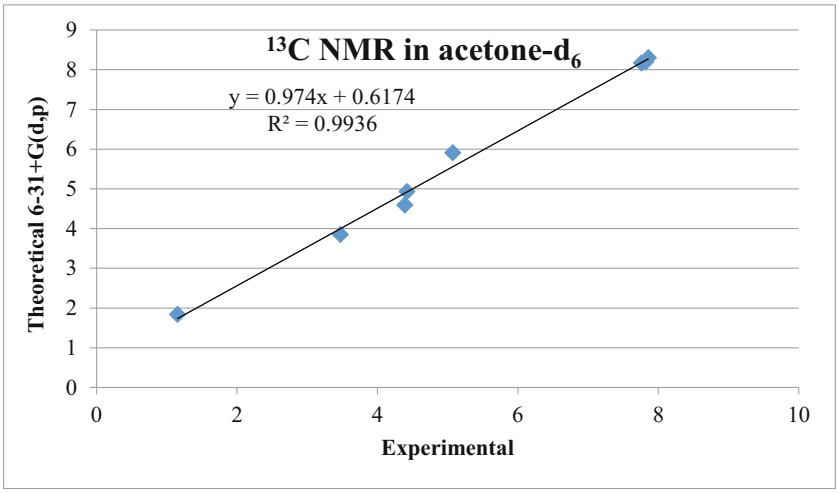

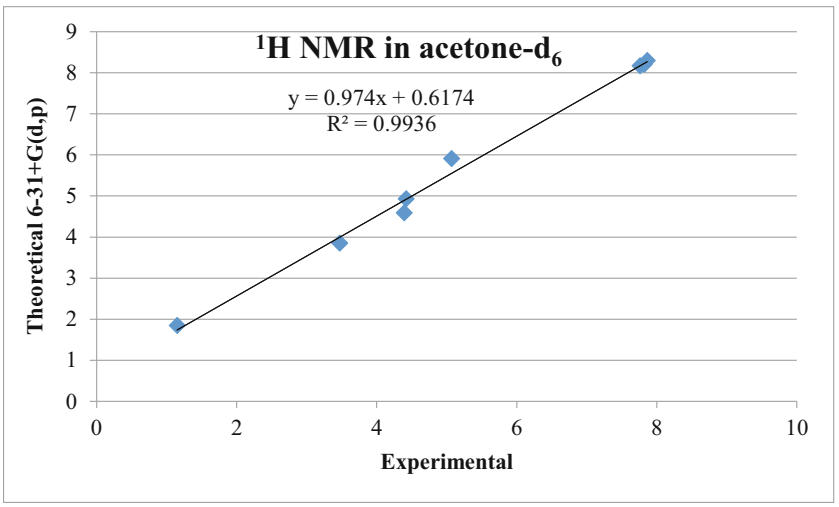

Fig. 4 The linear regression between experimental and calculated ^{1}H and ^{13}C NMR data of **3a**

the B3LYP/6-31+G(d,p) method. The theory showed the presence of two intramolecular hydrogen bonding in optimized structure **3a**. The DFT-simulated spectra of **3a** were in reasonably good agreement with the experimental spectra.

Supplementary Information The online version contains supplementary material available at https://doi.org/10.1007/s11224-020-01698-3.

Authors' contributions Maryam Khalili Foumeshi: conceptualization, formal analysis, investigation, resources, software, validation, visualization. Hossein Paghandeh: conceptualization, formal analysis, investigation, resources, software, validation, visualization. Hamid Saeidian: conceptualization, formal analysis, investigation, resources, software, validation, visualization, writing—review and editing.

Data availability The online version contains supplementary material available at https://doi.org/10.1007/s11224-020-01698-3.

Compliance with ethical standards

Conflict of interest The authors declare that they have no conflict of interest.

Code availability Not applicable.

References

1. Guina J, Merrill B (2018). J Clin Med 7:1–22
2. Votaw VR, Geyer R, Rieselbach MM (2019). McHugh RK Drug alcohol depend 200:95–114
3. Song MX, Deng XQ (2018). J Enzyme Inhib Med Chem 33:453–478
4. Sudhapriya N, Manikandan A, Rajesh Kumar M (2019). Perumald PT Bioorg Med Chem Lett 29:1308–1312
5. Haldar AJM, Chhajed SS, Mahapatra DK, Dadure KM (2017). Int J Curr Pharm Res 9:195–200
6. Thakrar S, Bavishi A, Radadiya A, Parekh S, Bhavsar D, Vala H, Pandya N, Shah A (2013). J Heterocyclic Chem 50:73–79
7. Verzijl GKM, Hassfeld J, de-Vries AHM, Lefort L (2020). Org Process Res Dev 24:255–260
8. Gatta E, Cupello A, Braccio MD, Grossi G, Ferruzzi R, Roma G, Robello M (2010). Neuroscience 166:917–923
9. Herpin T, Kirk KGV, Salvino JM, Yu ST, Labaudiniere RF (2000). J Comb Chem 2:513–521
10. Tiihonen J, Suokas JT, Suvisaari JM, Haukka J, Korhonen P (2012). Arch Gen Psychiatry 69:476–483

11. Dolda M, Lib C, Gilliesc D, Leucht S (2013). Eur Neuropsychopharmacol 23:1023–1033
12. Aasth P, Navneet K, Anshu A, Pratim S, Dharm K, Kumar E (2013). Res J Chem Sci 3:90–103
13. Garoufis A, Kitos AA, Lymperopoulou S, Nastopoulos V, Plakatouras JC, Ypsilantis K (2015). J Mol Struct 1079:473–479
14. El-Gaml KM (2014). J Org Chem 4:14–19
15. Wang LZ, Li XQ, An YS (2015). Org Biomol Chem 13:5497–5509
16. Jaafar Z, Chniti S, Sassi AB, Dziri H, Marque S, Lecouvey M, Gharbi R, Moncef M (2019). J Mol Struct 1195:689–701
17. Tehrani MB, Emani P, Rezaei Z, Khoshneviszadeh M, Ebrahimi M, Edraki N, Mahdavi M, Larijani B, Ranjbar S, Foroumadi A, Khoshneviszadeh M (2019). J Mol Struct 1176:86–93
18. Akın S, Demir EA, Colak A, Kolcuoglu Y, Yildirim N, Olcay B (2019). J Mol Struct 1175:280–286
19. Blanch NM, Chabot GG, Quentin L, Scherman D, Bourg S, Dauzonne D (2012). Eur J Med Chem 54:22–32
20. John J, Thomas J, Dehaen W (2015). Chem Commun 51:10797–10806
21. Crowley JD, McMorran DA (2012). Top Heterocycl Chem 28:31–84
22. Guha PM, Phan H, Kinyon JS, Brotherton WS, Sreenath K, Simmons JT, Wang Z, Clark RJ, Dalal NS, Shatruk M, Zhu L (2012). Inorg Chem 51:3465–3477
23. Hosseinnejad T, Ebrahimpour F, Fattahi B (2018). RSC Adv 8: 12232–12259
24. Dommerholt J, Schmidt S, Temming R, Hendriks LJA, Rutjes FPKT, Van-Hest JCM, Lefeber DJ, Friedl P, Van-Delft FL (2010). Angew Chem Int Ed 49:9422–9425
25. Tron GC, Pirali T, Billington RA, Canonico PL, Sorba G, Genazzani AA (2008). Med Res Rev 28:278–308
26. Agalave SG, Maujan SR, Pore VS (2011). Chem Asian J 6:2696–2718
27. Gil MV, Arevalo MJ (2007). O Lopez Synthesis 11:1589–1620
28. Alizadeh M, Mirjafary Z, Saeidian H (2020). J Mol Struct 1203: 127405–127415
29. Bonyad SR, Mirjafary Z, Saeidian H, Rouhani M (2019). J Mol Struct 1187:164–170
30. Taheri E, Mirjafary Z, Saeidian H (2018). J Mol Struct 1157:418–424
31. Paghandeh H, Saeidian H (2018). J Mol Struct 1157:560–566
32. Saeidian H, Vahdati S, Mirjafary Z, Eftekhari B (2018). B RSC Adv 8:38801–38807
33. Saeidian H, Sadighian H, Abdoli M, Sahandi M (2018). J Mol Struct 1157:560–566
34. Mirjafary Z, Ahmadi L, Moradi M, Saeidian H (2018). RSC Adv 8: 38801–38807
35. Saeidian H, Sadighian H, Arabgari M, Mirjafary Z, Ayati SE, Najafi E, Moghaddam FM (2018). Res Int Chem 44:601–612
36. Frisch MJ, Trucks GW, Schlegel HB, Scuseria GE, Robb MA, Cheeseman JR, Zakrzewski VG, Montgomery JA, Jr Stratmann RE, Burant JC, Dapprich S, Millam JM, Daniels AD, Kudin KN, Strain MC, Farkas O, Tomasi J, Barone V, Cossi M, Cammi R, Mennucci B, Pomelli C, Adamo C, Clifford S, Ochterski J, Petersson GA, Ayala PY, Cui Q, Morokuma K, Salvador P, Dannenberg JJ, Malick DK, Rabuck AD, Raghavachari K, Foresman JB, Cioslowski J, Ortiz JV, Baboul AG, Stefanov BB, Liu G, Liashenko A, Piskorz P, Komaromi I, Gomperts R, Martin RI, Fox DJ, Keith T, Al-Laham MA, Peng CY, Nanayakkara A, Challacombe M, Gill PMW, Johnson BG, Chen W, Wong MW, Andres JL, Gonzalez C, Head-Gordon M, Replogle ES, Pople JA (2013) Gaussian 09. Gaussian, Inc, Wallingford
37. Wolinski K, Hinton JF, Pulay P (1990). J Am Chem Soc 112:8251–8260
38. Naeimi H, Nejadshafiee V (2014). New J Chem 38:5429–5435
39. Zhou Z, Parr RG (1990). J Am Chem Soc 112:5720–5724
40. Gocen T, Bayarı SH, Guven MH (2017). J Mol Struct 1150:68–81
41. Parr RG, von Szentpaly L, Liu S (1999). J Am Chem Soc 121: 1922–1924
42. Parr RG, Yang W (1984) J Am Chem Soc 106:4049–4050